

## Ultrasonic Attenuation and Dispersion in Xenon near Its Critical Point\*

Peter E. Mueller, † Don Eden, ‡ and Carl W. Garland  
*Department of Chemistry and Center for Materials Science and Engineering,  
 Massachusetts Institute of Technology, Cambridge, Massachusetts 02139*  
 and

R. C. Williamson  
*Massachusetts Institute of Technology, Lincoln Laboratories, Lexington, Massachusetts 02173*  
 (Received 12 May 1972)

The sound velocity and attenuation of xenon near its critical point have been measured with a pulsed acoustic interferometer which incorporates phase-sensitive detection and signal averaging. Accurate data could be obtained over the frequency range from 0.4 to 7 MHz in spite of the very large attenuation. Results are given in detail along a near-critical isochore and are also reported along several isotherms.

### I. INTRODUCTION

Ultrasonic investigations of a simple fluid near its critical point can provide equilibrium information about the thermodynamic behavior and dynamical information about critical relaxation processes.<sup>1,2</sup> At sufficiently low frequencies, the sound velocity will equal the static adiabatic value  $u(0) = (\rho\kappa_S)^{-1/2}$  where  $\rho$  is the mass density and  $\kappa_S$  is the adiabatic compressibility. Thus, along the critical isochore  $u(0)$  should go to zero asymptotically as  $\epsilon^{\alpha/2}$ , where  $\epsilon = |T - T_c|/T_c$  and  $\alpha$  is the critical exponent which describes the divergence of  $C_v$ .<sup>1</sup> A variety of low-frequency resonance methods have been used recently to determine the limiting-velocity behavior near the critical points of He,<sup>3</sup> Ar,<sup>4</sup> and Xe.<sup>5</sup> In most cases the resonant cavity has an appreciable vertical height, and density gradients due to gravity must be taken into account.<sup>6</sup>

The present investigation was motivated by the need for much better experimental data characterizing the dynamical behavior in the critical region. Ultrasonic absorption and velocity dispersion were measured in the frequency range from 0.4 to 7 MHz along two near-critical isochores for  $T > T_c$ , along both the liquid and the vapor side of the coexistence curve for  $T < T_c$  and along several isotherms. Xenon was chosen because it has no internal degrees of freedom whose relaxation might obscure the critical behavior and because it has a convenient critical temperature ( $T_c = 16.59^\circ\text{C}$ ) and pressure ( $P_c = 57.636\text{ atm}$ ).<sup>7</sup> In addition, the early acoustic work on xenon by Chynoweth and Schneider<sup>8</sup> indicated a considerable frequency dependence for the velocity near the critical point. A wide variety of other measurements have been made in the critical region of xenon, and these aid in the interpretation of our results. In particular, there are excellent PVT data<sup>7</sup> and good  $C_v$  measurements.<sup>9</sup> Recent light-scattering results give

the thermal diffusivity,<sup>10</sup> the correlation range and the isothermal compressibility,<sup>11</sup> the heat-capacity ratio  $C_p/C_v$ ,<sup>12</sup> the surface tension, and the shear viscosity.<sup>13</sup> Hypersonic velocity and attenuation have been determined from Brillouin spectra.<sup>12,14</sup>

It is worthwhile to summarize the ultrasonic results of Chynoweth and Schneider<sup>8</sup> since they provide a background and comparison for the present work. Velocity data over a temperature range from 15 to 19 °C showed a sharp cusplike minimum at about 16.8 °C, which is 0.2 °C above the accepted value of  $T_c$ . In the immediate vicinity of the velocity minimum, a dispersion of ~6% was reported between the velocities at 0.25 and 1.25 MHz. Attenuation values were given only for 0.25 MHz, since the interferometric pattern was badly distorted at higher frequencies. It was, however, mentioned that the attenuation per wavelength appeared to be almost independent of frequency near the critical point.

The presence of velocity dispersion and very large critical attenuation is related to the behavior of the transport properties near a critical point. Recently, Kawasaki<sup>15</sup> has used the mode-mode coupling formalism<sup>16</sup> to predict the detailed behavior of sound propagation when the dominant mechanism is the decay of a sound mode into two heat modes. He gives not only the temperature behavior but also the magnitude of the reduced velocity dispersion and the critical sound absorption. Kawasaki's theory, which deals with the problem in terms of a complex bulk viscosity, is closely related to the early work of Fixman, who developed his theory in terms of a complex frequency-dependent specific heat. Indeed, Mistura<sup>17</sup> and Garland, Eden, and Mistura<sup>18</sup> have derived the Kawasaki results using a modification of the basic Fixman model.

Our velocity and absorption data along the critical isochore for  $T > T_c$  have already been ana-

lyzed<sup>18,19</sup> quite successfully in terms of mode-mode coupling theory. The present paper will give a more detailed account of that work (including a discussion of the choice of the reduced temperature  $\epsilon$ ), will present data obtained along the co-existence curve and along various isotherms, and will comment on the possible effects of gravity.

## II. EXPERIMENTAL METHOD

A cross-sectional view of the ultrasonic interferometer cell is shown in Fig. 1. The two transducers were matched 1-MHz X-cut quartz transducers, which were polished for overtone use. The upper one could be moved vertically by rotating a precision micrometer thread in a captured piston. This permitted an accurate variation in the acoustic path length from less than 1 mm up to 2 cm. The total volume of the cell (but not its internal shape) was independent of the position of the upper transducer. The temperature of the cell was measured with a West model CT quartz thermometer. The pressure was measured with a Dynisco model No. PT119H strain-gauge pressure transducer whose diaphragm was located at a level 1 mm above the lower transducer. A small magnetically driven stirrer mounted just below the lower transducer was used to stir the xenon during all the measurements. Limited tests indicated that the results were insensitive to whether the system was stirred or not. The entire cell was immersed in a large bath of hydraulic fluid, whose temperature could be regulated to within  $\pm 1$  m°C. Complete details are given elsewhere.<sup>20</sup>

It is obviously very important to know the temperature and pressure accurately and with high resolution. By counting the beat frequency of the quartz thermometer for 10 sec, a resolution of 0.1 m°C was achieved. The absolute accuracy of this thermometer, as calibrated by the manufacturer, should have been  $\pm 0.01$  °C. However, our calibration at the triple point of water showed that there were large zero-point corrections. Initially, the calibration correction  $[T(\text{true}) - T(\text{obs})]$  was 0.135 °C. After 16 months, during which the isochore measurements were made, this correction had increased to 0.145 °C. After another year, during which time no experiments on xenon were performed, the correction had changed from 0.145 to 0.264 °C. Over a period of 3 months during which most of the isotherm measurements were made, the correction increased from 0.264 to 0.268 °C. It is presumed that the zero-point shift changed gradually during the periods of measurement. Unfortunately, this cannot be proven conclusively since calibration of the quartz thermometer was not feasible during a run.

The pressure transducer had a full-scale rating of 1500 psi and was excited by a very stable

10-V dc power supply. The output of the transducer (3 mV/V full scale) was measured with a Leeds and Northrup K-3 potentiometer. The maximum resolution for pressures near the critical pressure was 0.1  $\mu\text{V}/\text{V}$ , which corresponds to 0.05 psi or approximately 5 parts in  $10^5$ . The accuracy of the pressure values depends on a combination of several error figures. The maximum error due to nonlinearity, hysteresis, and nonrepeatability was about 0.15% of full scale. (Hysteresis resulted in an accumulated shift in the zero point to higher values.) There was also an error introduced by changes in the temperature of the transducer, which was mounted in the same temperature bath as the ultrasonic etalon. For a 1 °C temperature change there can be a zero shift of 0.3  $\mu\text{V}/\text{V}$  and a shift in the sensitivity which is equivalent to another 0.3  $\mu\text{V}/\text{V}$  for a full-scale pressure reading. Along the critical isochore the expected value of  $(\partial P/\partial T)_\rho$  is 0.0350 mV/V. Thus an uncertainty of 2% in this value would not be unreasonable. Along an isotherm the pressure

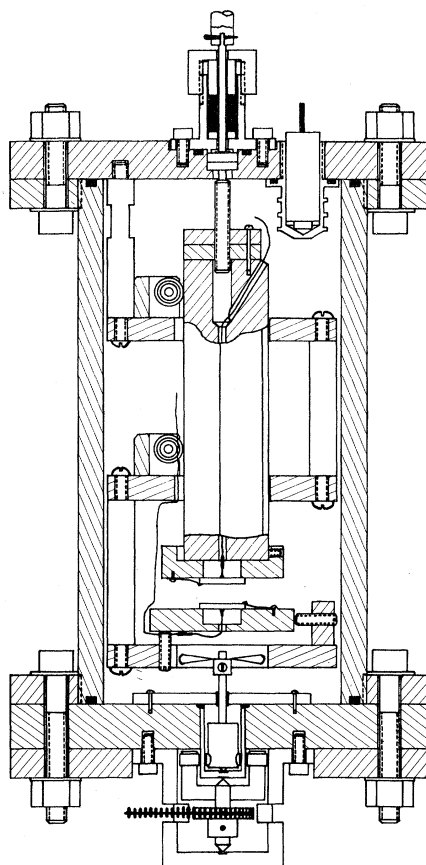


FIG. 1. Ultrasonic interferometer cell. In actual operation, aluminum blocks (not shown) were installed to fill most of the "dead volume." The internal height of the cell is 22 cm.

changes were more accurate since the temperature was constant and the pressure excursions were small. Hysteresis amounted to less than  $0.1 \mu\text{V}/\text{V}$  for any isotherm. The most annoying characteristic of bonded strain-gauge transducers is an aging effect. When left under a deforming stress the zero output can drift significantly; Lastovka and Feke<sup>21</sup> have determined a  $3.4\%/yr$  drift in the zero point for a similar model strain-gauge transducer. However, there has been no assessment of the effects of aging for the transducer used in this experiment.

The density for an isochore was related to the quantity  $(\partial P/\partial T)_\rho$  along the isochore by using the PVT data of Habgood and Schneider.<sup>7</sup> Since the variation of  $dP/dT$  along the coexistence curve is very well established, it was possible to calibrate the transducer during an isochore run (taking into account the effect of temperature on the sensitivity). Then an evaluation of  $(\partial P/\partial T)_\rho$  above  $T_c$  determined the density to within 1%.

The very large signal attenuation near the critical point limits the accuracy of ultrasonic velocity and absorption measurements if traditional pulse techniques are used. For this reason a phase-sensitive-detection scheme which incorporates signal averaging was developed. Accurate measurements of velocity and absorption could be made with this new method even when the attenuation was as large as  $0.40 \text{ Np/wavelength}$  (a typical value near the critical point). A complete description of this technique and an illustration of its application to xenon has been given elsewhere.<sup>22</sup> The more precise point-by-point procedure described previously<sup>22</sup> was carried out at each frequency for a given thermodynamic state of the system. Then the temperature or the mean density was changed and the sequence was repeated. Measurements of velocity with absolute accuracies of  $\pm 0.2\%$  and of attenuation with accuracies of  $\pm 2\%$  were routine. Better results could be obtained under favorable conditions. Diffraction corrections were negligible, and the signal was very seldom noise limited. The principal problem was caused by phase-coherent rf leakage. Because of the very narrow-band amplification used in this experiment, it was possible to work at frequencies lower than the 1-MHz fundamental of the quartz transducers. The receiving network had a good response at exciting frequencies of 0.4 and 0.55 MHz, and the phase-detection circuitry rejected the 1-MHz signal very effectively.

After completion of all experiments a sample of xenon was withdrawn from the cell. An analysis by gas-chromatographic techniques and flame photometry (performed by the New England Analytical Laboratory) showed that the only impurities present were 13-ppm air and 5-ppm methane. There

was no evidence of heavy-molecular-weight substances.

### III. RESULTS

In a simple fluid there is a classical sound absorption which can be described by the Navier-Stokes (NS) equation<sup>23</sup>

$$\alpha_\lambda(\text{NS}) = \frac{\pi\omega}{u^2} \left( \frac{4}{3}\eta + \xi_0 + \frac{\Lambda(C_v^{-1} - C_p^{-1})}{\rho} \right), \quad (1)$$

where  $\alpha_\lambda \equiv \alpha \cdot \lambda$  is the amplitude attenuation per wavelength,  $u$  is the sound velocity at frequency  $\omega$ ,  $\eta$  is the shear viscosity,  $\xi_0$  is the normal "non-relaxing" bulk viscosity which is assumed to have approximately the same magnitude as the shear viscosity,<sup>12,24</sup>  $\Lambda$  is the thermal conductivity, and  $C_v$  and  $C_p$  are the specific heats at constant volume and pressure. Although the shear viscosity and the thermal conductivity are weakly divergent, the term in the large parentheses is numerically quite small, and the total attenuation is much greater than the NS value near the critical point. For example,  $\alpha_\lambda$  at 1 MHz is over 1000 times  $\alpha_\lambda(\text{NS})$ . However, the  $\alpha_\lambda(\text{NS})$  value predicted by Eq. (1) can make a significant contribution far from the critical point where the critical ultrasonic attenuation due to the relaxing bulk viscosity  $\xi(\omega)$  is very small. In essence, we have divided the attenuation into a background value  $\alpha_\lambda(\text{NS})$  which involves the non-critical  $\xi_0$  and a value  $\alpha_\lambda(\text{crit})$  which is related to  $\xi(\omega)$ , the critical contribution to the bulk viscosity. All  $\alpha_\lambda$  values reported below are critical values, i. e., observed values corrected by subtracting the small  $\alpha_\lambda(\text{NS})$  contribution.<sup>18</sup> Classical sound dispersion due to a divergent  $\Lambda/\rho C_v$  term (i. e., deviation from adiabatic conditions) is completely negligible.<sup>20</sup>

Figure 2 shows the temperature variation of the 1-MHz sound velocity along two near-critical isochores and in the coexisting phases for temperatures near  $T_c$ . The smooth curve was obtained by interpolation from Chynoweth and Schneider's data at 0.75 and 1.25 MHz.<sup>8</sup> The mean density in their rather tall cell was equal to the critical density, but since their measurements were made at the bottom of the cell the local density must have been greater than  $\rho_c$ . In all these runs, the velocity minima occur above  $16.59^\circ\text{C}$ , the value which is usually cited as the critical temperature. Chynoweth and Schneider's velocity minima were at  $16.79^\circ\text{C}$  for 0.25 MHz,  $16.85^\circ\text{C}$  for 0.75 MHz, and  $16.91^\circ\text{C}$  for 1.25 MHz. In the present work, the velocity minimum was not a function of frequency. For the filling density  $\rho = 0.95\rho_c$ , the minimum velocity occurred at  $16.90^\circ\text{C}$ ; for  $\rho = 1.01\rho_c$ ,  $T_{\text{min}} = 16.953^\circ\text{C}$ . All temperature differences  $\Delta T$  used in Fig. 2 and elsewhere in this paper correspond to  $(T - T_{\text{min}})$ , where  $T_{\text{min}}$  is the temperature

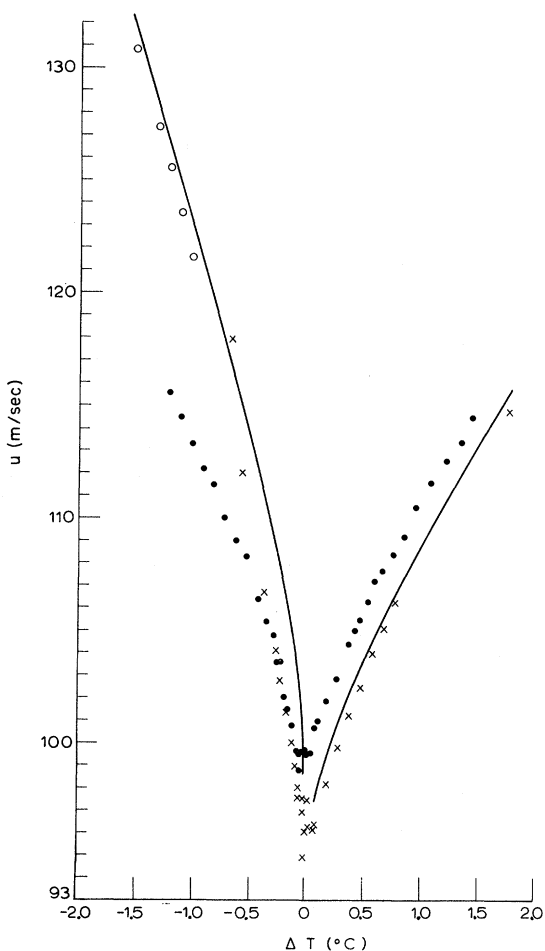


FIG. 2. The 1-MHz velocity along near-critical isochores. The crosses represent data obtained at a mean filling density of  $1.01\rho_c$ ; below  $T_c$  these data refer to the liquid. The circles represent data obtained at a mean filling density of  $0.95\rho_c$ ; open circles are used for the liquid and closed circles for the vapor and supercritical fluid. The solid line represents the behavior in the liquid and supercritical fluid obtained by interpolation of the data of Chynoweth and Schneider (see text).

of the velocity minimum.

Figure 3 shows the critical sound attenuation per wavelength at 1 MHz as a function of  $\Delta T$  for the same two isochores. The smooth curve is the result reported by Chynoweth and Schneider<sup>3</sup> at 0.25 MHz, the only frequency at which they were able to obtain attenuation results. Their  $\alpha_\lambda$  values show roughly the same variation as the present 1-MHz values but are considerable larger than they should be.

The velocity and attenuation values for all frequencies studied at  $\rho = 1.01\rho_c$  are given in Table I. The smooth-curve variation of  $\alpha_\lambda$  along this almost critical isochore and along the liquid side of the coexistence curve is shown in Fig. 4 for all fre-

quencies up to 3 MHz. Note that these  $\alpha_\lambda$  values become almost independent of  $\omega$  near  $T_c$ . The peak  $\alpha_\lambda$  values at 1 and 3 MHz correspond to attenuations  $\alpha$  of 393 and 1215 dB cm<sup>-1</sup>, respectively.

Velocity and attenuation measurements have also been made along several near-critical isotherms. Figure 5 gives the pressure dependence of the 1-MHz velocity for isotherms at 16.73, 16.84, 16.96, and 17.136 °C. The pressure is given in units of mV/V, which represents the direct reading of the pressure transducer. As discussed previously the absolute value of the pressure during any given run is unknown since there are zero shifts and thermal effects. In constructing Fig. 5, the pressures of the velocity minima were adjusted to occur at pressures which correspond to an extension of the vapor-pressure line.<sup>4</sup> In addition to the isotherms shown in Fig. 5, a very extensive set of data were obtained at 21.99 °C from an initial pressure of 65 atm ( $\rho > \rho_c$ ) to a final pressure of 1 atm. The minimum 1-MHz velocity along this supercritical isotherm was 129.4 m sec<sup>-1</sup>. This is in excellent agreement with the interpolated value of 129.7 m sec<sup>-1</sup> at that temperature on the  $1.01\rho_c$  isochore run. Furthermore, the value of

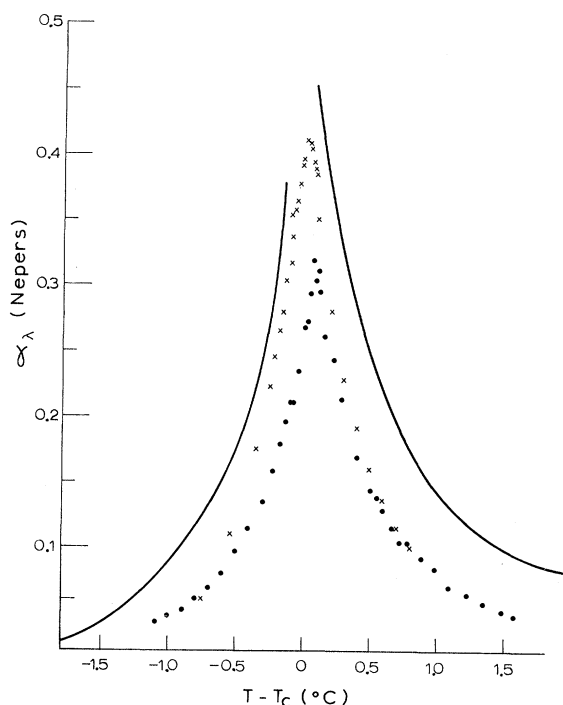


FIG. 3. Critical attenuation per wavelength at 1 MHz along near-critical isochores. The symbols are the same as those used in Fig. 2. Note that below  $T_c$  the crosses represent data in the liquid phase while the circles are for the vapor phase. The solid line represents the 0.25-MHz result reported by Chynoweth and Schneider.

176.6 m sec<sup>-1</sup> obtained by extrapolation to zero pressure at 21.99 °C agrees very well with the calculated ideal gas value of  $(\gamma RT/M)^{1/2} = 176.5$  m sec<sup>-1</sup>. Although the 16.96 °C isotherm has the lowest and sharpest minimum, the largest frequency range was studied along the 17.136 °C isotherm. Numerical data for this isotherm are tabulated elsewhere,<sup>25</sup> but smooth-curve plots of the velocity dispersion and critical absorption are given in Figs. 6 and 7.

## IV. DISCUSSION

The attenuation and velocity dispersion along the 1.01ρ<sub>c</sub> isochore above T<sub>min</sub> have been analyzed previously<sup>18,19</sup> in terms of the mode-mode coupling theory. The actual experimental data are reported here for the first time (see Table I). We shall not repeat the substance of the previous data analysis or review the modified theoretical expressions derived for the case of large dispersion near a

TABLE I. Velocity and critical attenuation per wavelength for a mean filling density ρ = 1.01ρ<sub>c</sub>. The temperature difference ΔT = T - 16.953 °C (see text).

ΔT	Velocity (m sec <sup>-1</sup> )						Attenuation per wavelength (Np)					
	0.4	0.55	1	3	5	7 MHz	0.4	0.55	1	3	5	7 MHz
19.783		159.93	159.10	159.15	159.24	159.04		0.0016	0.0003	0.0006	0.0016	0.0017
14.782		151.91	151.48	151.44	151.70	151.46		0.0009	0.0010	0.0014	0.0018	0.0029
9.782		142.68	141.99	142.04	141.92	142.09		0.0013	0.0014	0.0035	0.0049	0.0062
7.282		136.73	136.15	136.09	136.71	136.00		0.0019	0.0024	0.0057	0.0098	0.0142
4.782		129.13	128.95	129.14	129.04	128.93		0.0031	0.0054	0.0136	0.0199	0.0281
3.782		125.35	125.17	125.47	125.47	125.39		0.0045	0.0081	0.0209	0.0321	0.0404
2.783		120.75	120.78	120.74	121.15	121.28		0.0088	0.0149	0.0366	0.0555	0.0617
1.782		114.88	114.83	115.32	115.80	115.49		0.0196	0.0320	0.0690	0.0921	0.1305
0.782		105.89	106.28	107.66	106.57			0.0710	0.1000	0.1621	0.1984	
0.682		104.66	105.14	105.95	110.28			0.0838	0.1167	0.1940	0.1949	
0.582		103.30	103.96	105.20	109.44			0.1002	0.1354	0.2058	0.1648	
0.482		101.94	102.51	104.62	107.11			0.1231	0.1604	0.2351	0.2599	
0.383		100.26	101.25	103.52	105.62			0.1518	0.1919	0.2701	0.2312	
0.283		98.54	99.84	100.71				0.1892	0.2293	0.3029		
0.183		96.61	98.21	100.37				0.2449	0.2812	0.3495		
0.082		94.35	96.37	103.09				0.3217	0.3521	0.3667		
0.075	92.94	94.05	96.12	103.10			0.3506	0.3630	0.3850	0.4738		
0.062	92.97	94.17	96.30	103.10			0.3519	0.3633	0.3897	0.4142		
0.050	92.92	93.88	96.22	101.81			0.3616	0.3714	0.3977	0.4248		
0.035	92.70	93.88	96.22				0.3613	0.3863	0.4048			
0.026		94.90	97.52	102.46				0.3349	0.3537	0.3746		
0.023	92.67	93.76	96.31				0.3780	0.3848	0.4092			
0.008	92.79	93.76	96.22				0.3758	0.3873	0.4096	0.4473		
0.001		95.55	97.52	103.10				0.3243	0.3516	0.3958		
-0.003	92.81	93.82	96.12	104.05			0.3866	0.3951	0.4122	0.4752		
-0.017		93.08	94.93	102.33				0.4210	0.4297	0.4131		
-0.019	93.37	94.67	96.86				0.3593	0.3731	0.3971	0.4585		
-0.028		95.35	97.61	102.46				0.3337	0.3578	0.3892		
-0.029	93.63	94.94	96.96	104.37			0.3580	0.3664	0.3941	0.4261		
-0.045	94.22	95.43	97.49	105.64			0.3411	0.3530	0.3790	0.4293		
-0.062		95.55	97.61	103.10			0.3391	0.3657	0.4216			
-0.063	94.01	95.92	98.00	105.96			0.3261	0.3411	0.3657	0.4211		
-0.077	95.23	96.41	98.20	104.05			0.3115	0.3260	0.3575	0.4098		
-0.093		96.06	98.20	104.62			0.3289	0.3550	0.3837			
-0.099	96.10	97.02	98.99	105.96			0.2868	0.3035	0.3377	0.4135		
-0.113	96.83	97.87	100.08	105.96			0.2721	0.2874	0.3184	0.3800		
-0.117		96.16	98.20	103.64				0.3280	0.3544	0.3996		
-0.142	97.93	98.86	100.82	105.39			0.2464	0.2639	0.3033	0.3697		
-0.169	98.91	99.68	101.40	105.39			0.2274	0.2474	0.2812	0.3474		
-0.194	99.86	100.68	101.97	106.28			0.2109	0.2251	0.2671	0.3390		
-0.221	100.61	101.52	102.82	106.28			0.1880	0.2085	0.2473	0.3352		
-0.263	102.13	102.74	104.16	106.91			0.1678	0.1823	0.2241	0.2977		
-0.359	105.30	105.82	106.75	109.46			0.1185	0.1380	0.1763	0.2572		
-0.558	110.99	111.46	112.08	114.54			0.0642	0.0761	0.1116	0.1806		
-0.759	115.47	116.72	118.13	120.77			0.0385	0.0437	0.0603	0.1149		

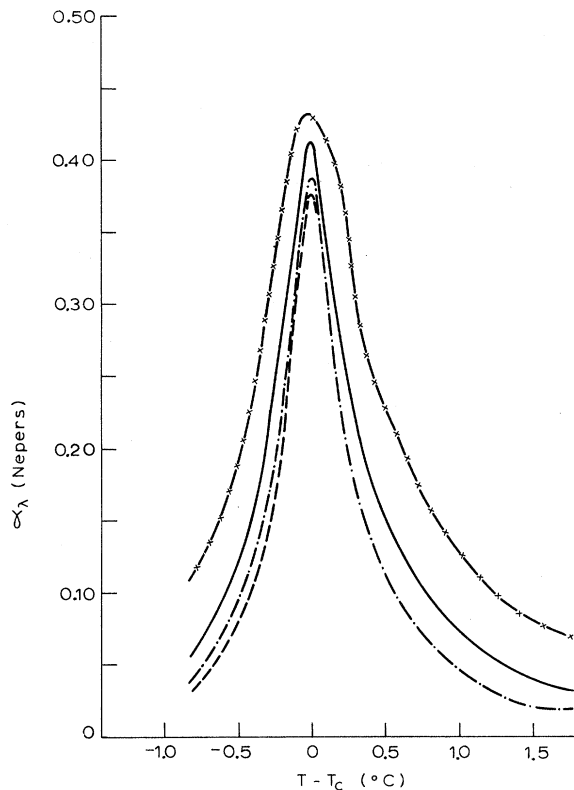


FIG. 4. Critical attenuation per wavelength for the isochore  $\rho = 1.01\rho_c$ . The smooth curves represent the  $\alpha_\lambda$  values given in Table I at 3 MHz ( $\times-\times-\times$ ), 1 MHz (solid line), 0.55 MHz ( $-\cdot-\cdot-\cdot$ ), and 0.40 MHz (dashed line).

critical point.<sup>19</sup> It will suffice to say that good agreement was obtained between theory and experiment for both our ultrasonic and the available hypersonic data.<sup>12,14</sup> This agreement was, however, obtained by taking 16.953 °C (the observed temperature of the velocity minimum) as the critical temperature for the analysis of all the ultrasonic data; i. e., the reduced temperature  $\epsilon$  corresponding to a data point on this isochore was taken as  $(T - T_{\min})/T_{\min}$ . This choice was based on the assumption, consistent with Eqs. (9)–(12) of Ref. 19, that  $u(\omega)$  will vary in the same qualitative manner as  $u(0)$  in the immediate vicinity of the critical point. Thus  $u(\omega)$  at a finite  $\omega$  is assumed to achieve its lowest value at the critical point. Nevertheless, it is unclear why this value of  $T_{\min}$  differs so greatly from the usually cited  $T_c$  value of 16.59 °C.

Systematic errors in the thermometer scale should be less than 5 m °C for the 1.01 $\rho_c$  isochore since the quartz thermometer was calibrated at the triple point both before and immediately after the run. The possibility that impurities are responsible does not seem consistent with the analyses carried out after the experiment was completed. Another explanation would seem to be density effects caused by gravity.<sup>6,26</sup> The vertical separation between the transducers was only a few millimeters for measurement near the critical point, and the density gradient between them would not be very large. However, the local density at the height of the lower (stationary) transducer can

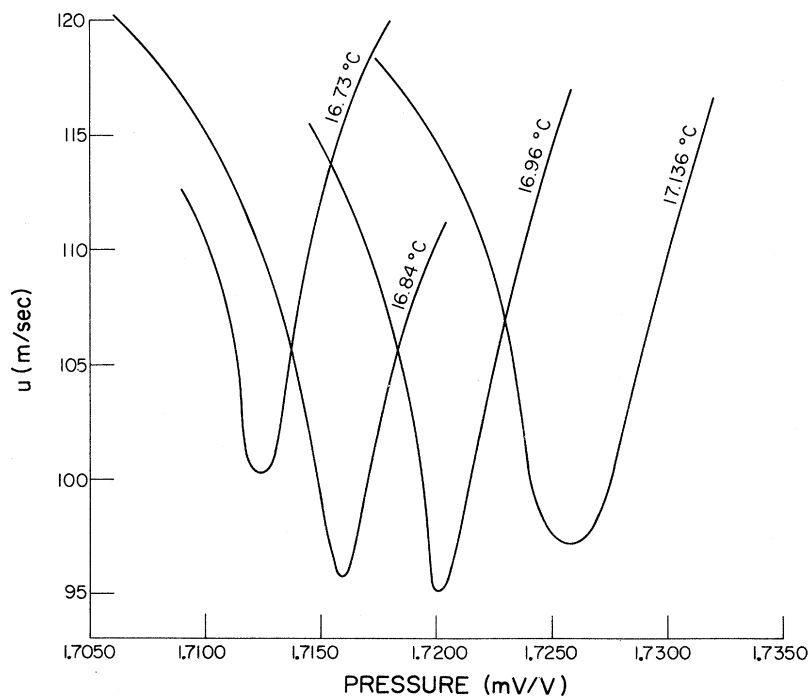


FIG. 5. The 1-MHz velocity along several isotherms. The pressure is in experimental units (see text).

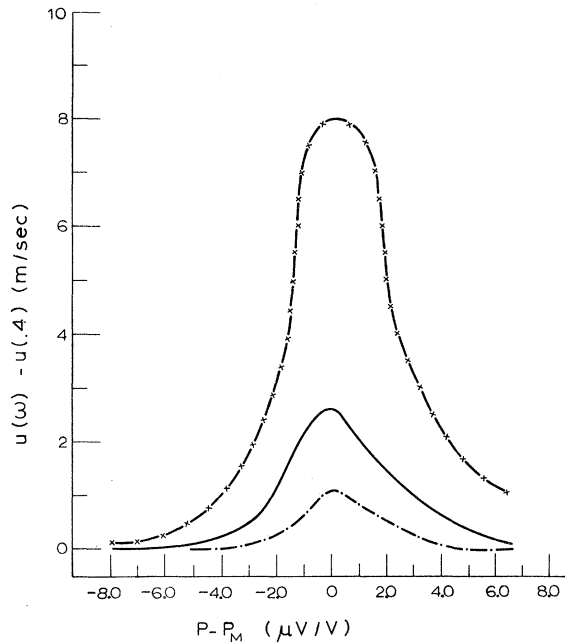


FIG. 6. Velocity dispersion along the 17.136 °C isotherm. The smooth curves represent the differences between velocities at 3 MHz (—x—x—), 1 MHz (solid line), and 0.55 MHz (— · — ·) and those at 0.40 MHz. The pressure difference is in experimental units relative to the pressure of the velocity minimum.

change with temperature since the transducer is not at the volumetric center of the quite complex cell. For the isochore in which the mean filling density was  $0.95\rho_c$ , the meniscus formed below the transducers and the local density at  $T_c$  was certainly less than  $\rho_c$ . For the isochore with a mean filling density of  $1.01\rho_c$ , the meniscus formed above the transducers and the local density at  $T_c$  could be appreciably greater than  $\rho_c$ . There are, however, two reasons that such density effects due to gravity should not amount to much. First of all, the filling procedure was such that the density was adjusted to give the lowest possible velocity at a temperature near  $T_c$ . The cell was then closed and the mean filling density was determined subsequently from  $(\partial P/\partial T)_\rho$ . Second and most important, Fig. 5 shows that the isotherm at 16.96 °C has a lower minimum value than any other. Although the local density at the level of the transducers is not known for these isotherms, it is obviously a monotonic function of the pressure. For the  $1.01\rho_c$  isochore, the 1-MHz velocities at 16.73, 16.84, 16.96, and 17.136 °C were 102.8, 100.1, 96.2, and 98.2 m sec<sup>-1</sup>, respectively. These values are quite close to the corresponding minimum values of 100.3, 95.6, 95.0, and 97.2 m sec<sup>-1</sup> shown in Fig. 5. Therefore, gravity effects do not seem to play a substantial role in

modifying the results obtained along the  $1.01\rho_c$  isochore. The final possibility is to challenge the assumption that  $u(\omega)$  at a finite frequency will have its lowest value at the critical point. However, the use of 16.59 °C as  $T_c$  in analyzing the ultrasonic data would require that a very strong increase in dispersion and decrease in critical attenuation must occur rather suddenly in the region between 16.59 and 16.95 °C. Such an effect could not be understood in terms of present mode-mode coupling theory. Indeed, the choice of  $T_c = 16.59$  °C for the analysis of our ultrasonic data along the  $1.01\rho_c$  isochore would largely destroy the reported agreement<sup>19</sup> between the ultrasonic results and both theory and hypersonic results. In summary, the use of  $T_{\min}$  for the critical temperature in the analysis of our isochore data seems to be an internally consistent choice which leads to agreeable results, but the reason that  $T_{\min}$  is 0.36 °C above the accepted  $T_c$  value is completely unclear (see note added in manuscript).

The attenuation data obtained below  $T_{\min}$  along the  $1.01\rho_c$  isochore can be analyzed in a manner exactly like that used above  $T_{\min}$ . It has been shown that  $\alpha_\lambda(\text{crit})$  above  $T_{\min}$  depends on the temperature and frequency through a single reduced variable  $\omega^* = \omega/\omega_D$ .<sup>18</sup> In that analysis, the characteristic frequency

$$\omega_D = (2\lambda/\rho C_p)\xi^{-2} \quad (2)$$

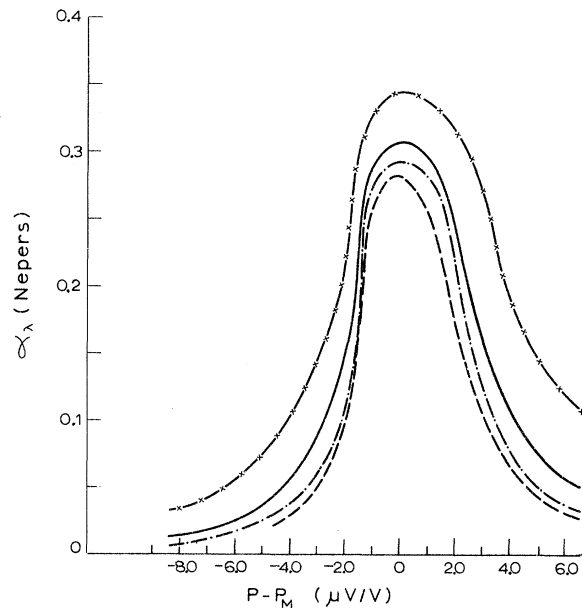


FIG. 7. Critical attenuation per wavelength on the 17.136 °C isotherm. The smooth curves represent the values at 3 MHz (—x—x—), 1 MHz (solid line), 0.55 MHz (— · — ·), and 0.40 MHz (dashed line). The pressure scale is the same as that used in Fig. 6.

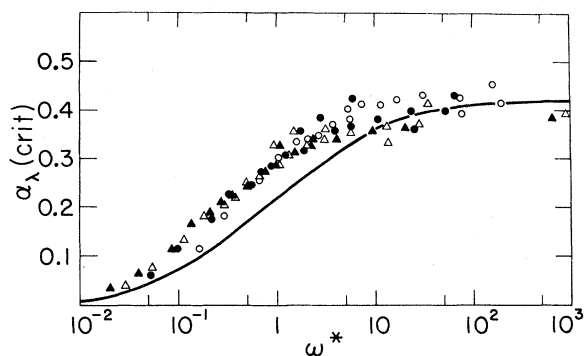


FIG. 8. Critical attenuation per wavelength along the  $1.01\rho_c$  isochore for  $T < T_{\min}$  as a function of reduced frequency  $\omega^* = \omega/\omega_D$ . Data are shown at 0.4 MHz (closed triangle), 0.55 MHz (open triangle), 1 MHz (closed dot), and 3 MHz (open dot), with  $\omega_D$  taken to be  $14.6 \times 10^{12} \epsilon^{1.87}$ . The smooth curve represents the variation of  $\alpha_\lambda$  observed above  $T_{\min}$  (see Ref. 18). The choice of  $\omega_D = 5.38 \times 10^{12} \epsilon^2$  would give equally good agreement among  $\alpha_\lambda$  values at different frequencies.

for thermal diffusion was represented by  $5.38 \times 10^{12} \epsilon^2 \text{ sec}^{-1}$  and  $\epsilon$  was taken to be  $|T - T_{\min}|/T_{\min}$ . If the same  $\omega_D$  expression is used for analyzing the data below  $T_{\min}$ , all  $\alpha_\lambda(\text{crit})$  values again lie on a common curve when plotted against  $\omega^*$ . Indeed, the  $\alpha_\lambda$  values for  $|T - T_{\min}| \leq 0.35^\circ\text{C}$  are almost symmetric about  $T_{\min}$  and the  $\alpha_\lambda(\text{crit})$ -vs- $\omega^*$  plot below  $T_{\min}$  is essentially identical to the plot above  $T_{\min}$  given previously.<sup>18</sup> However, this choice of  $\omega_D$  is not unique. One could also assume that all data below  $T_{\min}$  were obtained in the coexisting liquid. If, for simplicity, the correlation lengths

in the coexisting vapor<sup>11</sup> are assumed to equal those in the liquid and recent data on the thermal diffusivity along the coexistence curve<sup>27</sup> are used,  $\omega_D$  can be represented by  $14.6 \times 10^{12} \epsilon^{1.87} \text{ sec}^{-1}$ . A plot of  $\alpha_\lambda(\text{crit})$  vs  $\omega^*$  based on this choice of  $\omega_D$  is shown in Fig. 8. Since the exponent 1.87 does not differ greatly from the previous choice of 2, the shape of the  $\alpha_\lambda$  variation does not change much, but all the  $\omega^*$  values are shifted down by a roughly constant multiplicative factor of  $\sim 0.28$ . Unfortunately, velocity dispersion cannot be analyzed in detail below  $T_{\min}$  since there are no reliable  $u(0)$  values. Roughly speaking, the dispersion between 0.55 and 3 MHz appears to be symmetric about  $T_{\min}$  although the velocities themselves are not.

The temperature variation of the low-frequency sound velocity along the critical isochore can be compared with other data by calculating the constant-volume heat capacity. The appropriate thermodynamic equation is

$$C_v = \frac{T(\partial P/\partial T)_v^2}{\rho^2 u^2(0)(1 - C_v/C_p)}, \quad (3)$$

where  $u(0)$  is the zero-frequency adiabatic sound velocity. The quantity  $(\partial P/\partial T)_v$  is well known along the critical isochore from the PVT work of Habgood and Schneider.<sup>7</sup> Near the critical point the quantity  $(1 - C_v/C_p)$  is very close to unity and can be determined from light-scattering intensity measurements.<sup>28</sup> Figure 9 shows the calculated variation in  $C_v$  as a function of  $\Delta T$  when  $u(0)$  is approximated by using the  $\sim 8$ -kHz velocity data of Kline and Carome,<sup>5</sup> the 0.25-MHz results of Chynoweth and Schneider,<sup>8</sup> and the present 0.55-MHz

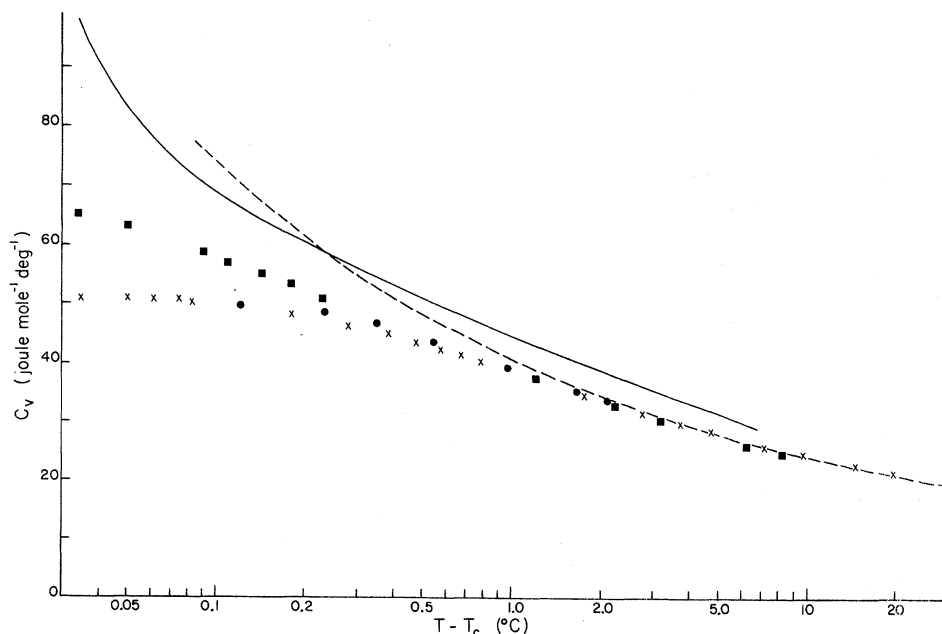


FIG. 9. Variation of  $C_v$  along the critical isochore. The direct calorimetric measurements of Edwards, Lipa, and Buckingham (Ref. 9) are represented by the solid line. The values calculated by Habgood and Schneider (Ref. 29) from PVT data are represented by the dashed line. The acoustic results are at  $\sim 8$  kHz (squares), 0.25 MHz (dots), and 0.55 MHz (crosses).

velocities. The solid line represents the static  $C_v$  values obtained from direct calorimetric measurements by Edwards, Lipa, and Buckingham.<sup>9</sup> The dashed line shows the  $C_v(T, \rho_c)$  variation calculated by Habgood and Schneider<sup>29</sup> from the ideal gas values  $C_v(T, 0)$  and their extensive  $PVT$  data. This technique is an excellent way to evaluate  $C_v$  far from the critical point, but the values close to  $T_c$  are overestimated. In each case for the acoustic data  $\Delta T$  was taken to be  $(T - T_{\min})$ , where  $T_{\min}$  was 16.67 °C for the data at 8 kHz, 16.79 °C for the data at 0.25 MHz, and 16.953 °C for the present data. The measurement of the resonance frequency of a 0.25-in.-high cell gave 8-kHz velocities which were systematically 1.4 m sec<sup>-1</sup> higher than the present 0.55-MHz values for  $\Delta T$  values between 3.78 and 7.28 °C. In this region, both the 0.55-MHz and the 8-kHz velocities should be effectively "zero-frequency" values. Since Kline and Carome have not included end corrections for their resonant system, their results could easily be in error by 1%. Therefore, we have reduced all of the 8-kHz velocities by 1.4 m sec<sup>-1</sup>.

At temperatures far from  $T_c$ , Fig. 9 shows that there is excellent agreement between the  $C_v$  values determined from the  $PVT$  measurements and the acoustic measurements. The calorimetric values appear to be systematically high by 3.5 J mole<sup>-1</sup> °C<sup>-1</sup>, which is close to the uncertainty in their absolute values.<sup>9</sup> Thus, all the results for  $C_v$  are consistent if the direct calorimetric values are reduced by ~3.5 J mole<sup>-1</sup> °C<sup>-1</sup>. As the critical point is approached,  $C_v$  as determined from sound-velocity measurements deviates from the results of static measurements when dispersion becomes appreciable. The "rounding" occurs over the widest  $\Delta T$  range for the 0.55-MHz data and over the smallest  $\Delta T$  range for the 8-kHz data. The effect of gravity on all these measurements is a complicating feature<sup>26,30</sup> which becomes especially important in the range  $\Delta T < 0.1$ . However, it can be shown that even at 8-kHz velocity dispersion will cause deviations from a limiting power-law behavior at a higher temperature than that at which gravity effects become significant. Incidentally, a power-law fit to the low-frequency velocities above  $\Delta T = 0.2$  gave ~0.2 for the critical exponent  $\alpha$  (uncorrected for gravity).

The velocity dispersion and attenuation shown in

Figs. 6 and 7 along a supercritical isotherm are typical of the results obtained along other isotherms. The analysis of such results in terms of mode-mode coupling theory is much more difficult than the analysis along an isochore for at least two reasons. First of all, the measurements were made as a function of pressure, and it would be necessary to use an equation of state to obtain  $u$  and  $\alpha_\lambda$  in terms of the density. Moreover, it is almost impossible to account for the density gradients in the system. (The shape of the cell is complicated and not known precisely enough to allow one to use an equation of state to predict the local density.) Thus very near the critical point the relation between  $P$  and  $\rho$  is not well defined. Second, the calculation of  $\omega_D$  is difficult because both the divergent and regular parts of the thermal diffusivity must be considered. The regular part of the thermal conductivity has a strong density dependence, and the density must be well known before this part can be estimated. Sengers and Keyes<sup>31</sup> have shown that the divergent part of the thermal conductivity obeys scaling along the critical isochore and along the coexistence curve. It seems reasonable that this scaling would hold anywhere near the critical point. If so, the critical contribution to  $\omega_D$  could be determined. In view of these difficulties, it does not seem worthwhile to attempt a mode-mode analysis of the dynamical behavior along the isotherms.

The lack of local-density information (or even absolute-pressure readings) is a serious impediment to the interpretation of isothermal data and prevents our establishing the critical temperature from our data without assuming that  $u(\omega)$  is a minimum at the critical point. It is most important to resolve this point, and simultaneous measurements of local density and ultrasonic velocity are now in progress.

*Note added in manuscript.* Recent measurements in the same cell using a standardized platinum resistance thermometer show that the critical temperature is 16.64 °C. Ultrasonic velocities at 0.6, 1, and 3 MHz all approach a minimum value at the critical point. The high values of  $T_{\min}$  reported in this paper and discussed in Sec. IV are almost completely due to systematic errors in the quartz thermometer used. Thus the validity of the analysis carried out in terms of  $|T - T_{\min}|$  is confirmed.

\*Research supported in part by the Advanced Research Projects Agency and in part by the National Science Foundation.

†Present address: Bell Telephone Laboratories, Allentown, Pa.

‡Present address: Department of Physics, New York University, New York, N.Y.

<sup>1</sup>C. W. Garland, in *Physical Acoustics*, edited by W.

P. Mason and R. N. Thurston (Academic, New York, 1970), Vol. 7, Chap. 2.

<sup>2</sup>D. Sette, in *Proceedings of the 1970 Varenna Conference on Critical Phenomena*, edited by M. S. Green (Academic, New York, 1971).

<sup>3</sup>M. Barmatz, *Phys. Rev. Letters* **24**, 661 (1970).

<sup>4</sup>J. Thoen, E. Vangeel, and W. Van Dael, *Physica* **52**, 205 (1971).

- <sup>5</sup>J. L. Kline and E. F. Carome (private communication).  
<sup>6</sup>M. Barmatz and P. C. Hohenberg, *Phys. Rev. Letters* **24**, 1225 (1970); M. Barmatz, in *Proceedings of Battelle Colloquium on Critical Phenomena, Gstaad, Switzerland, 1970* (McGraw-Hill, New York, 1972).  
<sup>7</sup>H. W. Habgood and W. G. Schneider, *Can. J. Chem.* **32**, 98 (1954).  
<sup>8</sup>A. G. Chynoweth and W. G. Schneider, *J. Chem. Phys.* **20**, 1777 (1952).  
<sup>9</sup>C. Edwards, J. A. Lipa, and M. J. Buckingham, *Phys. Rev. Letters* **20**, 496 (1968); H. H. Schmidt, J. Opdycke, and C. F. Gay, *ibid.* **19**, 887 (1967).  
<sup>10</sup>D. L. Henry, H. L. Swinney, and H. Z. Cummins, *Phys. Rev. Letters* **25**, 1170 (1970); H. L. Swinney, D. L. Henry, and H. Z. Cummins, *J. Phys. (Paris) Suppl.* **33**, C1-81 (1972).  
<sup>11</sup>M. Giglio and G. B. Benedek, *Phys. Rev. Letters* **23**, 1145 (1969); I. W. Smith, M. Giglio, and G. B. Benedek, *ibid.* **27**, 1556 (1971); G. B. Benedek, J. B. Lastovka, M. Giglio, and D. Cannell, in *Proceedings of Battelle Colloquium on Critical Phenomena, Gstaad, Switzerland, 1970* (McGraw-Hill, New York, 1972).  
<sup>12</sup>D. S. Cannell and G. B. Benedek, *Phys. Rev. Letters* **25**, 1157 (1970).  
<sup>13</sup>J. Zollweg, G. Hawkins, I. W. Smith, M. Giglio, and G. B. Benedek, *J. Phys. (Paris) Suppl.* **33**, C1-135 (1972).  
<sup>14</sup>H. Z. Cummins and H. L. Swinney, *Phys. Rev. Letters* **25**, 1165 (1970).  
<sup>15</sup>K. Kawasaki, *Phys. Rev. A* **1**, 1750 (1970); **3**, 1097 (1971).  
<sup>16</sup>L. P. Kadanoff and J. Swift, *Phys. Rev.* **166**, 89 (1968).  
<sup>17</sup>L. Mistura, in Ref. 2.  
<sup>18</sup>C. W. Garland, D. Eden, and L. Mistura, *Phys. Rev. Letters* **25**, 1161 (1970).  
<sup>19</sup>D. Eden, C. W. Garland, and J. Thoen, *Phys. Rev. Letters* **28**, 726 (1972).  
<sup>20</sup>P. E. Mueller, Ph.D. thesis (Massachusetts Institute of Technology, 1969) (unpublished).  
<sup>21</sup>J. Lastovka and G. Feke (private communication).  
<sup>22</sup>R. C. Williamson and D. Eden, *J. Acoust. Soc. Am.* **47**, 1278 (1970).  
<sup>23</sup>K. F. Herzfeld and T. A. Litovitz, *Absorption and Dispersion of Ultrasonic Waves* (Academic, New York, 1959).  
<sup>24</sup>P. Gray and S. A. Rice, *J. Chem. Phys.* **41**, 3689 (1964).  
<sup>25</sup>D. Eden, Ph.D. thesis (Massachusetts Institute of Technology, 1971) (unpublished).  
<sup>26</sup>P. C. Hohenberg and M. Barmatz, *Phys. Rev. A* **6**, 289 (1972).  
<sup>27</sup>D. Henry, Ph.D. thesis (Johns Hopkins, 1970) (unpublished); I. Smith (private communication); T. Lim (private communication).  
<sup>28</sup>The Landau-Placzek ratio can be used for  $C_v/C_p$ , but light-scattering data give this quantity at hypersonic frequencies. It is better to determine  $C_p - C_v$  from the light-scattering value of  $(\partial\rho/\partial\mu)_T$  and iterate.  
<sup>29</sup>H. W. Habgood and W. G. Schneider, *Can. J. Chem.* **32**, 164 (1954).  
<sup>30</sup>H. H. Schmidt, *J. Chem. Phys.* **54**, 3610 (1971).  
<sup>31</sup>J. V. Sengers and P. H. Keyes, *Phys. Rev. Letters* **26**, 70 (1971).

## Diffraction Scattering of Picosecond Light Pulses in Absorbing Liquids\*

R. I. Scarlet†

Laboratory of Atomic and Solid State Physics, Cornell University, Ithaca, New York 14850  
 (Received 9 March 1972)

A mode-locked neodymium-glass laser with a fast shutter was used to study light scattering from an absorbing liquid. Two equal high-intensity beams from the laser intersected at a small angle in the liquid, and the resulting stimulated diffractive scattering was observed. Scattering was found on two time scales: a fast effect, developing within the 10-psec duration of a mode-locked laser pulse, and a slow effect requiring many nanoseconds to develop. An analysis is presented which shows the slow effect to be a combination of stimulated thermal Rayleigh scattering and stimulated thermal Brillouin scattering. The fast effect is explained as a result of saturation of the absorbing liquid in an interference pattern.

### I. INTRODUCTION

Molecular scattering of light, in the form of Rayleigh, Rayleigh-wing, and Brillouin scattering, is now known in both spontaneous and stimulated versions. The stimulated scattering was first demonstrated for Brillouin scattering by Chiao, Townes, and Stoicheff.<sup>1</sup> Characteristic of their experiment, and almost all of those that followed, is the use of two light beams passing through the same region of the material being studied. One

beam is a high-intensity laser beam, and the second, at some angle to the first, is of very low intensity.

In the sample, then, is an interference pattern of electromagnetic fields caused by the two beams. The fields are coupled to some property of the sample (density, polarizability, etc.). Hence, the condition of the sample is altered—in stimulated Brillouin scattering (SBS), for example, a sound wave is induced. The changed properties of the sample, acting back on the light through the dielec-